



3D numerical investigation of roadway bridge response under hydrodynamic forces and local scour in stiff clay and sand foundations



Nurul Shafrina Atika Saiful Nizam, Nordila Ahmad*, Zuliziana Suif, Jestin Jelani
Faculty of Engineering, National Defence University of Malaysia, Malaysia

Abstract

Bridges are critical components of transportation networks but are highly vulnerable to failure during extreme flood events, particularly due to hydrodynamic forces and local scour. This study quantitatively evaluates the effects of flood velocity and scour depth on bridge pier displacement for two representative soil conditions: very stiff clay (Ground Type B) and medium-dense sand (Ground Type C). A 3D finite-element model incorporating non-linear p-y springs was developed in CSI Bridge to represent soil-structure interaction (SSI). A total of 192 simulations were performed across flood velocities of 2–16 m/s and scour depths ranging from 0DF to 2DF. The results show that pier displacement increases systematically with both velocity and scour, with medium-dense sand exhibiting up to 30% higher displacement than very stiff clay at severe flood conditions (0.07 m vs. 0.06 m). These findings highlight the importance of soil stiffness in governing pier response under extreme hydrodynamic loading. While the study does not address debris impact, flow directionality or additional hydraulic parameters, the outcomes provide valuable insight for improving foundation design and incorporating SSI considerations into flood-resilient bridge engineering.

This is an open-access article under the CC BY-SA license.



Keywords:

Displacement;
Hydrodynamic Force;
Medium Dense Sand;
Scour Depth;
Very Stiff Clay;

Article History:

Received: October 25, 2025
Revised: December 1, 2025
Accepted: December 16, 2025
Published: January 8, 2026

Corresponding Author:

Nordila Ahmad
Civil Engineering Department,
National Defence University of
Malaysia, Malaysia
Email: nordila@upnm.edu.my

INTRODUCTION

Bridges are essential elements within the modern transportation infrastructure system and play a critical role in maintaining the growth of the economy. The functionality of these structures requires consideration, especially in the context of extreme natural occurrences. Adherence to the current design criteria of bridges requires empirical modelling expertise, as well as a deeper insight into the susceptibility of the bridge to natural hazards. In light of the different factors responsible for the collapse of a bridge, hydraulic processes like local scour, channel migration, and flood loads have been recognized as the predominant factors in determining the functionality of the transportation systems [1].

Scour, described as the erosion of soil surrounding a bridge foundation, has continued to be the primary cause of bridge failures. In the period from 1980 to 2012, scour was responsible for over half of the total number of bridge collapses in the United States, a fact which substantially surpasses other causes [2]. Owing to the aggravation of climate change and global warming, floods have become more erratic, unpredictable, and devastating in nature [3]. The devastating floods that ravaged Western Europe in July 2021 have aptly depicted the serious socioeconomic impact of such disasters, despite the advanced flood defense structures available in Germany, Belgium, and the Netherlands [4][5].

Although much attention has been given to the seismic response of bridges, fewer research works have been conducted concerning flood hazards, particularly the joint impact of hydrodynamics and local scour on the response of bridge structures [3], [6]. In fact, most research works have considered the hydrodynamics impact on a bridge as well as the soil condition, but without incorporating both simultaneously, although both soil condition and hydrodynamics impact have a vital relationship in determining the response of a bridge. The comparison indicated in the Table 1 shows the lack of attention given to the impact of different soil properties, which affects the response of a bridge as the velocity of the flood increases, along with the level of local scour.

In addition, cohesion, density, and permeability of the soil can play a very significant role in deciding the foundation stability of a bridge, particularly in the context of a flood event, as a result of reduced lateral support because of scour. The fact that a comparison study on the behavior of bridges on different soil types subject to increasingly higher flood speeds has not been conducted can be identified as a very significant limitation. Accordingly, the research objective of this study is to analyze the behavior of a bridge model as it responds to the rise of flood levels on two representative soil categories, which are very stiff clay soil and medium dense sand. The research highlights the importance of SSI in flood response, as it aims to inform on the impact of soil properties on the displacement of bridge structures under extreme hydraulic loads. The research is expected to contribute to the development of more robust bridge structures as it seeks to improve current engineering practice.

The comparison drawn within Table 1 emphasizes the fact that most of the available research has considered the hydrodynamics as well as the geotechnical behavior of bridge systems independently, without accounting for the joint impact of these factors on the bridge response. Most of the available research has considered the individual effects of scour in bridges as well as hydrodynamics. However, very limited research has considered a realistic SSI model within flood fragility assessments. The inability of the available research to provide a comprehensive interface between soil behavior, scour, as well as hydrodynamics has contributed to the limitations in determining the accuracy of the flood vulnerability of bridge systems. The research gaps mentioned have been overcome within this research since it provides a comprehensive assessment of bridge displacement, as well as stability, based on the impact of varying flood

velocities, as well as scour depths, for two different soil conditions, namely very stiff clay and medium dense sand.

SCOUR MECHANISM

The phenomenon of bridge scours during flood events is widely acknowledged as a significant factor contributing to bridge failure. The rapid increase in water velocity from upstream to downstream during a flood. The movement of water from the surface to the bottom around bridge piers is caused by this phenomenon, as shown in Figure 1. The primary mechanism by which a scour hole is formed is the displacement of sediments surrounding the foundations due to the downward flow of water. The generation of the horseshoe vortex and wake vortex is attributed to variations in flow depths. The formation of a scour hole of a specific depth is a direct consequence of this phenomenon. The occurrence of bridge scour at bridge foundations is a widespread phenomenon, with its depth being influenced by various factors, including water velocity, pier dimensions, and sediment types. The significance of integrating bridge scour into a finite element model (FEM) is paramount, as it profoundly influences the overall stability of the bridge system [7].

The erosion of soil around bridge piers and foundations leads to the uncovering of the foundation, causing a subsequent reduction in the soil's strength and stiffness contribution. This phenomenon has resulted in an increased length of unsupported foundation, reduced lateral stiffness, strength, buckling resistance, and factor of safety against stability, and heightened vulnerability of the entire bridge structure. The scouring of bridge foundations leads to a reduction in the bed level, which in turn causes an elevation in the flow-induced load on the bridge.

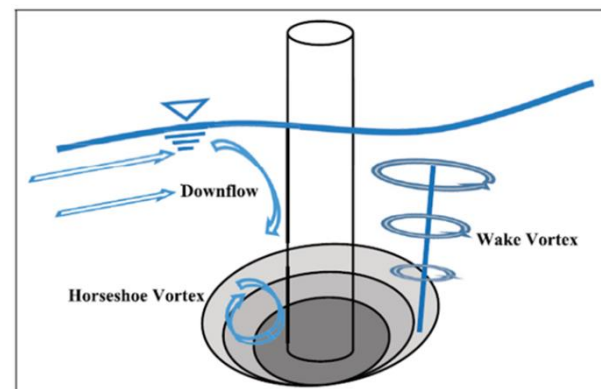


Figure 1. Occurrence of the scour hole during the flood [7]

Table 1. Comparative summary of previous studies on bridge performance under flood and multi-hazard conditions, highlighting soil consideration and existing research gaps.

Authors	Focus of Study	Hazards Considered	Soil Consideration		Limitation
Ameh Fioklou et al. (2019) [8]	Fragility analysis of bridges under multi-hazard events	Seismic and flood hazards	Partial (uniform soil type)		No differentiation between clay and sand response under scour conditions
Nofal & Van de Lindt (2020) [9]	To extend the typical single-variable flood vulnerability function, which is based solely on flood depth, to a multi-variate function that considers both flood depth and duration.	Flood	Not considered		Ignored the influence of soil stiffness and foundation type.
Argyroudis et al. (2021) [10]	combinations of hydraulic (flood and scour) and seismic hazards	Floods and earthquakes	Clayey sand (Ground type C)		Only clay, no comparison for soil types.
Anisha et al. (2022) [3]	Flood fragility of RC bridges under various loading scenarios	Flood	Soil taken random variable from previous studies.		The specific soil type was not identified.
Stefanidou et al. (2022) [11]	Multi-hazard fragility of bridges	Earthquake and Flood	Soil type C		Only one type of soil types.
Guo et al. (2023) [12]	Assess bridge failure due to scour and barge impacts	Flood and Collision	Barge	Two layers of soil which are soft clay, and hard clay	Soil type and scour depth were not considered in the comparative analysis.
Zhang et al. (2024) [13]	Simulate the hydrodynamic-SSI of shallow bridge piers	Flood		Soil taken random variable from previous studies.	The specific soil type was not identified.
Jianguo Wang et al. (2025) [14]	Dynamic response of bridge piers to the impact of flash flooding, particularly focusing on the effects SSI and scour around pile foundations	Flash flooding and scour		The research considers various soil types, specifically three different sandy soils: compact sand, dense sand, and very dense sand, to analyze their effects on SSI with respect to bridge piers subjected to flash flooding	Only sand, no comparisons for soil types.
Cristopher et al. (2025) [15]	Assess seismic fragility under time-varying scour	Earthquake and Scour		Not considered	Ignored the influence of soil stiffness and foundation type.
Current study (N. Shafrina et al.)	Bridge response under flood hazards	Hydrodynamic forces (flood) and local scour - simultaneously	Very stiff clay and medium dense sand (explicit comparison)		Addresses the gap by integrating soil-structure interaction with hydrodynamic loading for quantitative flood fragility evaluation

This is in addition to the factors mentioned earlier. This study examines the effects of flood events, particularly local scour, on the behavior of bridges against flood load. The focus is on understanding the immediate outcomes of these events. Figure 2 presents a cross-sectional view of the bridge in the transverse direction, depicting scenarios both with and without scouring [3].

According to [10], the interaction between water-soil and the bridge constitutes a significant element in understanding the failure modes of flood-critical bridges. The bridge components may be affected, including the foundation being vulnerable to scouring and hydraulic forces impacting the footing, pier, and/or abutment. In

certain scenarios, the significant depth of water may cause it to overflow onto the deck, resulting in considerable hydraulic forces on the superstructure. These effects are widely recognized as fundamental.

HYDRODYNAMIC FORCES

The hydrodynamic forces exerted on a bridge pier during a flood are essential factors that significantly impact the stability and resilience of the structure. The velocity and turbulence of floodwaters play a crucial role in determining the impact of hydrodynamic forces, as higher velocities can significantly amplify their effects.

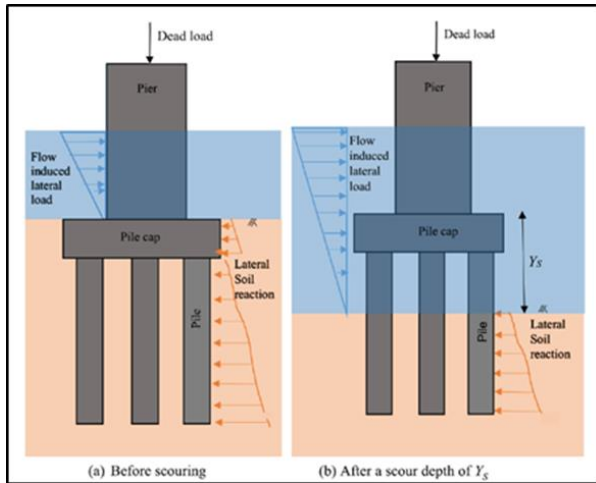


Figure 2. Influence of scour on stability of pier foundation [3]

The forces at play consist of drag and lift components, with the shape and surface characteristics of the pier playing crucial roles. Efficient designs are known to minimise drag, while variations in water pressure surrounding the pier generate lift forces. The occurrence of vortex shedding, which involves the formation of vortices in the wake of the pier, introduces a level of intricacy to the forces involved. The presence of debris transported by floodwaters has the potential to impede and modify flow patterns, thereby exacerbating dynamic interactions. The presence of hydrodynamic forces additionally contributes to the phenomenon of scouring around the base of the pier, which in turn has a significant impact on its foundation. The structural response encompasses the application of dynamic loading, which induces cyclic stresses. If not adequately addressed during the design phase, these stresses can accumulate over time and potentially result in fatigue and failure.

Based on the [16], the distribution of hydrodynamic force $F(y)$, (kg/m^2) on the pier at a height y from the bed level can be expressed:

$$F(y) = 52. K. V(y)^2 \quad (1)$$

$V(y)$ denotes the velocity of the water current at a height y in m/s , K is the constant that depends on the shape of the pier (circular pier = 0.66). $V(y)^2$ in the equation linearly varies from zero (at the deepest scour) to the square of the maximum velocity (at the free surface of water), as shown in Figure 3(a). The distribution of hydrodynamic force is shown in Figure 3(b). The hydrodynamic force as per (1) was applied on the structure to perform the nonlinear finite element analysis.

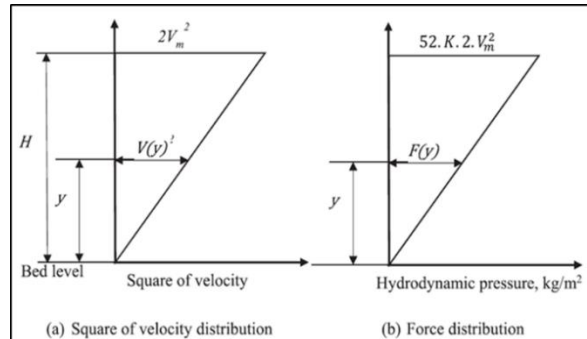


Figure 3. Velocity and hydrodynamic force distribution [3]

METHOD

For the flood hazard, eight flood velocity recorded on very stiff clay and medium dense sand are selected as outcrop motion for the analyses. The intensity measure (IM) used for the flood hazard was the scour depth and flood water level. The flood velocity was equal to 2, 4, 6, 8, 10, 12, 14, 16 m/s , and applied separately for each scour depth, i.e. 0DF, 1DF, 1.5DF, 2DF simulating the sequential occurrence of the two hazards. Therefore, a total of 192 analyses were studied, i.e. 4 Sc levels \times 3 flood levels \times 8 flood velocity \times 2 soil conditions. The depth of foundation (Df) is 1.2 m and scouring are assumed to occur when the floodwater level reaches 1 m above ground level (G.L). Mesh convergence analysis has been conducted to ascertain numerical accuracy as well as efficiency. The progression of the mesh continued until the difference in the highest pier displacement from one mesh to the next was below 5% while refining the mesh. The objective of the sensitivity analysis has been to determine the significance of influential parameters, such as soil properties, velocity, as well as scour, on the total displacement of the bridge. The results have further assisted in determining the paramount factors responsible for the susceptibility of the bridge to flooding. The overall research framework is illustrated in Figure 4, which summarizes the key steps in the modelling and analysis process, including data input, model validation, parametric simulation, and data analysis.

Numerical Modelling

The material and geometrical data is provided in this study, based on the available as-built construction information. Data was estimated from a retrofitting project conducted. The bridge consists of three main spans measuring 18 m each, supported by two piers that are firmly anchored in the riverbed of the Langat River. The bridge measures 54 m in length and 13 m in width.

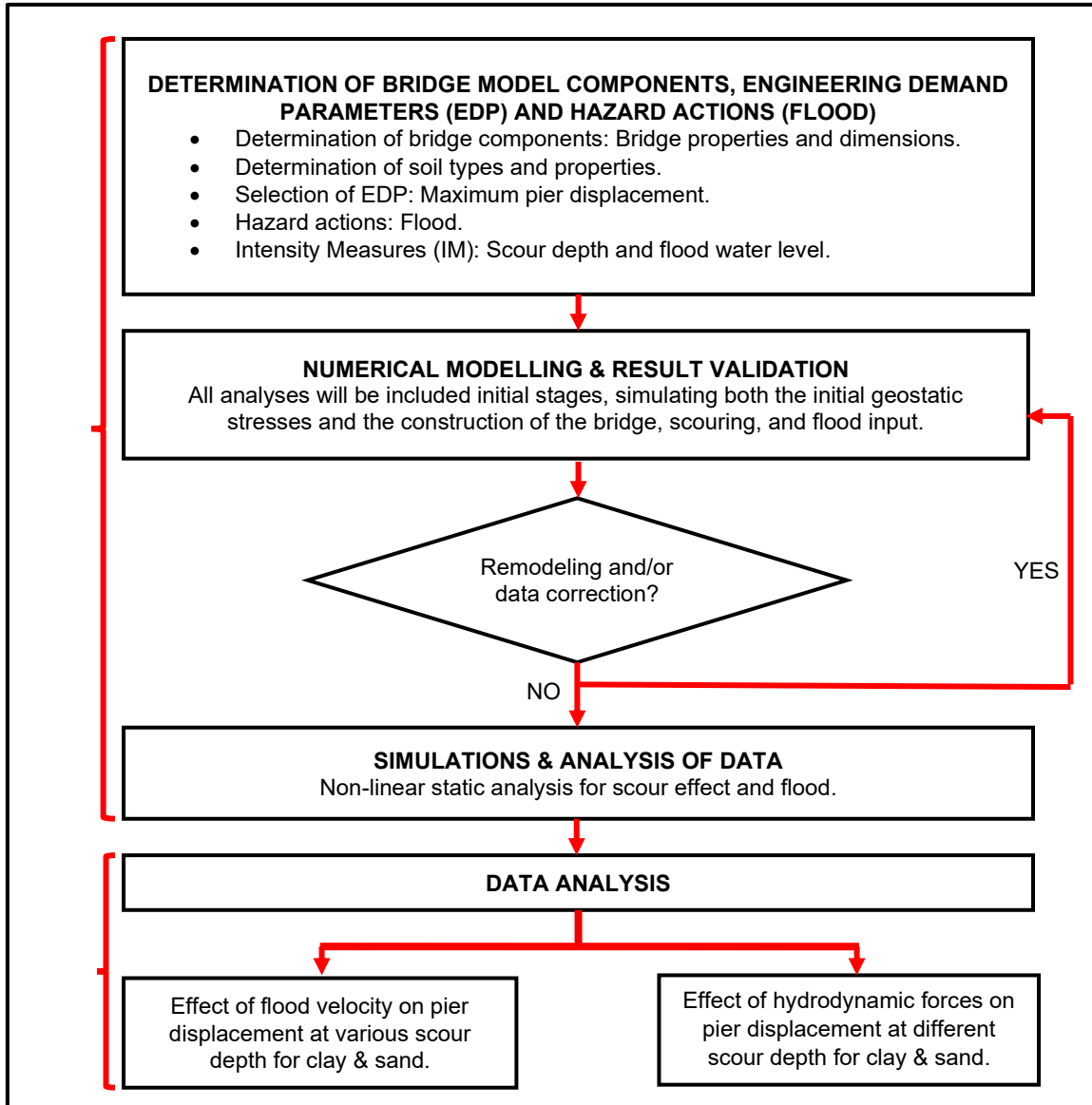


Figure 4. Flow Chart of Research Design and Procedure

The bridge is constructed with two traffic lanes, each measuring 3.5 m, and road shoulders on both sides measuring 3 m each. It is supported by cantilever beams at the upstream part of the bridge. The abutments have a height of 11 m, while the footing measures 1 meter in thickness and spans a length of 5.5 m. The piers have a circular shape, measuring 1.2 m in diameter and standing at a height of 8 m. The mechanical characteristics of the superstructure were acquired through destructive testing conducted during a retrofitting project for the structure. According to Eurocode 2, the estimated concrete grade of the bridge deck is equivalent to C25/30.

The bridge's material model is linear elastic. The bridge exhibits a non-porous behavior. In this study, ground types B (very stiff clay) and C (medium dense sand) have been

utilized as defined by Eurocode 8 – Part 1, and these classifications provide critical insights into the observed behaviors of bridge piers under hydrodynamic forces and local scour. It is assumed that the soil profile are very stiff clay and medium dense sand, and the soil properties will be referenced from the literature [17][18]. The simulation runs were expanded to include two different soil conditions which is very stiff clay and medium dense sand. For each soil type, a total of 96 simulation runs were executed. The extensive approach led to a total of 192 simulation runs, enabling a comprehensive examination of the bridge's vulnerability in various environmental conditions with different flood water levels and scour depths, to capture a diverse range of scenarios that accurately represent real-life flood events. The bridge model shown in Figure 5 was

created using CSI Bridge software. This bridge is constructed using reinforced concrete while the material properties of the bridge are Poisson's Ratio is 0.2, and Young's Modulus is 3×10^7 kN/m². The hydrodynamic forces were computed according to [16] as in (1). The temperature of the water was 20°C. This study did not consider traffic loads, as it was assumed that the bridge would be closed to traffic under this specific combination of loads. Hydrodynamic forces were only applied on the areas of the bridge that were not impacted by debris. In other words, there is no predicted interaction between the debris and the hydrodynamic loads. This is because, according to the Australian code loads resulting from debris include the hydrodynamic loads' contribution; hence, in order to prevent repetition, these loads are excluded when debris is present. The loads were computed based on the length of each individual component and were implemented in the model as evenly distributed loads.

For modeling SSI, the p-y link element is a widely used tool in geotechnical engineering and finite element analysis software. It is utilised to accurately model the lateral SSI in the analysis of deep foundation systems, like piles [19]. According to [20], the soil-foundation-structure interaction is modeled by applying nonlinear springs along the length of the equivalent pile. In this study, the soil-foundation interaction is simulated by assigning nonlinear p-y springs to the nodes throughout the whole length of the equivalent pile at intervals of 0.3 m.

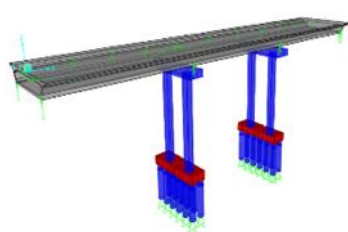


Figure 5. Bridge model in CSI Bridge

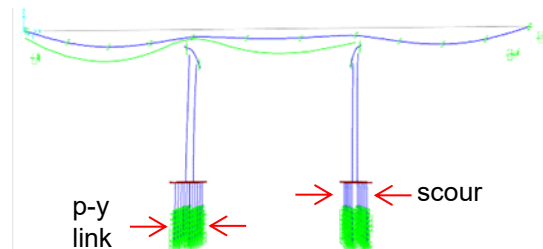


Figure 6. P-y spring and scour depth assigned

The determination of this spacing is based on the findings of early parametric research, which demonstrated that the hydrodynamic behaviour of the sample bridge remained unchanged when the foundation was simulated using lateral springs spaced at intervals of 0.3 m or less (equivalent to 1 ft). Scour occurs when a section of the bridge foundation, or the corresponding pile, experiences a loss of sideways support from the surrounding soil. In order to simulate the decrease in lateral support, the p-y springs are eliminated until a depth of scour is reached, which is measured from the top of the comparable pile or ground surface. The selected distance between two consecutive soil springs, which is equal to 0.3 m, is a shared factor for the depths of erosion that are being examined in this study. Thus, three soil springs, specifically those with values of 4, 6, and 8, are extracted from the top of the pile to simulate scour depths of 1.2 m, 1.8 m, and 2.4 m, respectively. As suggested by [20], hinge supports are placed at the ends of the comparable piles. Figure 6 shows the piles that have been assigned with the p-y link.

RESULTS AND DISCUSSION

Effect of the Flood Velocity on the Pier Displacement at Various Scour Depth

Figure 7 shows the relationship between flood velocity (V) and the pier displacement (δ) at various scour depths (Df) for every flood water level. With the increase in flood velocity, there is a noticeable rise in the displacement of the bridge piers for all scour depths.

The data indicate a clear positive correlation between velocity and displacement, with higher velocities and deeper scour depths producing greater pier movement. To quantify this relationship, a power-law regression was fitted to the data for each scour depth and soil type:

$$\delta = a \cdot V^b \quad (2)$$

where a and b are regression coefficients determined for each combination of scour depth and soil type. The regression results yielded high coefficients of determination ($R^2 > 0.95$) for all cases, indicating strong predictive accuracy. For example, for 2Df in clay, $a = 0.0012$ and $b = 1.15$, while for sand at 2Df, $a = 0.0014$ and $b = 1.18$, highlighting that displacement grows slightly faster with velocity in sand than in clay.

At higher velocities, the rate of increase in displacement reaches a point where it becomes more consistent and steady. Figure 7 (a), (b) and (c) illustrate the relationship between flood velocity and pier displacement for a bridge foundation on very stiff clay at varying scour depths (0df, 1df,

1.5df, 2df). As the flood velocity increases from 0 to 16 m/s, the displacement of the pier consistently rises across all scour depths. The data shows that deeper scour levels at 2df result in significantly higher displacements compared to shallower ones, 0df. For instance, at 16 m/s, the displacement at 2df is approximately 0.06 m, while at 0df, it is around 0.01 m. This indicates that as scour depth increases, the structural stability of the bridge piers decreases, leading to greater displacement under similar hydrodynamic forces. The trend is particularly noticeable at higher velocities, emphasizing the compounded risk of flooding and scouring on bridge integrity. While [Figure 7\(d\), \(e\) and \(f\)](#) depicts the effect of flood velocity on pier displacement for a bridge foundation on medium dense sand, also at varying scour depths. Like the stiff clay foundation, an increase in flood velocity results in higher pier displacement across all scour depths. However, the overall displacement values for stiff clay are lower than those for medium dense sand at the same velocities and scour depths. For example, at 16 m/s, the displacement for 2df in medium dense sand is about 0.07 m, whereas for stiff clay it is 0.06 m.

This indicates that stiff clay foundations offer slightly better resistance to hydrodynamic forces compared to medium dense sand. Nevertheless, the pattern of increasing displacement with both velocity and scour depth remains consistent, highlighting the vulnerability of the bridge piers to these factors [\[21\]\[22\]](#). [\[23\]](#) stated that flow velocity affects local scour depth. The greater the velocity, the deeper the scour. There is a high probability that scour is affected by whether the flow is subcritical or supercritical.

Statistical interpretation based on standard deviation, as well as 95% confidence intervals, has confirmed the expected variability of displacement being more apparent at higher velocities as well as larger scour depths, specifically for the medium dense sand.

The proposed regression model can be utilized as a predictive tool to determine pier displacement based on the impact of different flood velocities as well as pier scour depths.

Effect of Hydrodynamic Force on Pier Displacement at Different Scour Depth

[Figure 8](#) shows the relationship between the hydrodynamic force with pier displacement for different flood water levels. As the load increases to 103.4 kN/m, the displacement of the clay increases to 0.02 m. There has been a significant 19% increase in displacement. The displacement experiences a significant increase of 36% for 1df,

with the value rising from 0.019 to 0.03 m. The displacement experiences a significant increase of 34% from 0.025 to 0.035 m at 1.5df, and a notable 17% increase from 0.03 to 0.04 m at 2df.

Next, the displacement at 1.62 kN/m for 0df in very stiff clay at water level 5 meter is initially 0.027 m, which later increases to 0.038 m at 103.4 kN/m. Displacement has increased by 30%. At 1df, the displacement shows a significant 35% increase, ranging from 0.029 to 0.045 m. The displacement presents a significant increase of 29% from 0.032 to 0.044 m at 1.5df, followed by a notable 22% increase from 0.03 to 0.04 m at 2df. The very stiff clay displacement at flood water level 7 m begins at 0.035 m with an initial load of 1.62 kN/m, and then increases to 0.046 m with a load of 103.4 kN/m. Displacement has increased by 26%. The displacement at 1df has increased by 30%, going from 0.037 m to 0.053 m. The displacement experiences a significant increase of 28% from 0.039 m to 0.054 m at 1.5df, followed by a 23% increase from 0.046 m to 0.06 m at 2df.

On the other hand, at water level 5 m. At 1df, the displacement has increased by 42%, ranging from 0.032 to 0.055 m. The displacement experiences a significant increase of 37% from 0.035 to 0.055 m at 1.5df, followed by a 30% increase from 0.041 to 0.059 m at 2df. Then, the medium dense sand displacement at flood water level 7 m begins at 0.037 m with an initial load of 1.62 kN/m and then rises to 0.056 m with a load of 103.4 kN/m. Displacement has been increased by 34%. The displacement at 1df increases by 37%, going from 0.04 m to 0.063 m. The displacement shows a significant increase of 35% from 0.042 m to 0.064 m at 1.5df, followed by a 30% increase from 0.049 m to 0.07 m at 2df.

The data clearly indicates that as scour depths increase, the absolute displacements also increase. It also shows that, at a maximum scour depth of 2.0df, the displacement becomes noticeably evident, indicating a catastrophic decrease in structural stability. These findings are consistent with the results presented in reference [\[22\]](#), which indicate that hydrodynamic loading can greatly increase the risk of bridge failure due to scour. This hazardous scenario can occur more frequently at commonly seen at high water levels. According to [\[24\]](#), ground type C is more plastic than ground type B where it shows more non-linear behavior and reaches the plastic limit condition. The sandy layers show mostly bilinear behavior and as indicated in the figure, need to be subjected to large load values to reach their ultimate state.

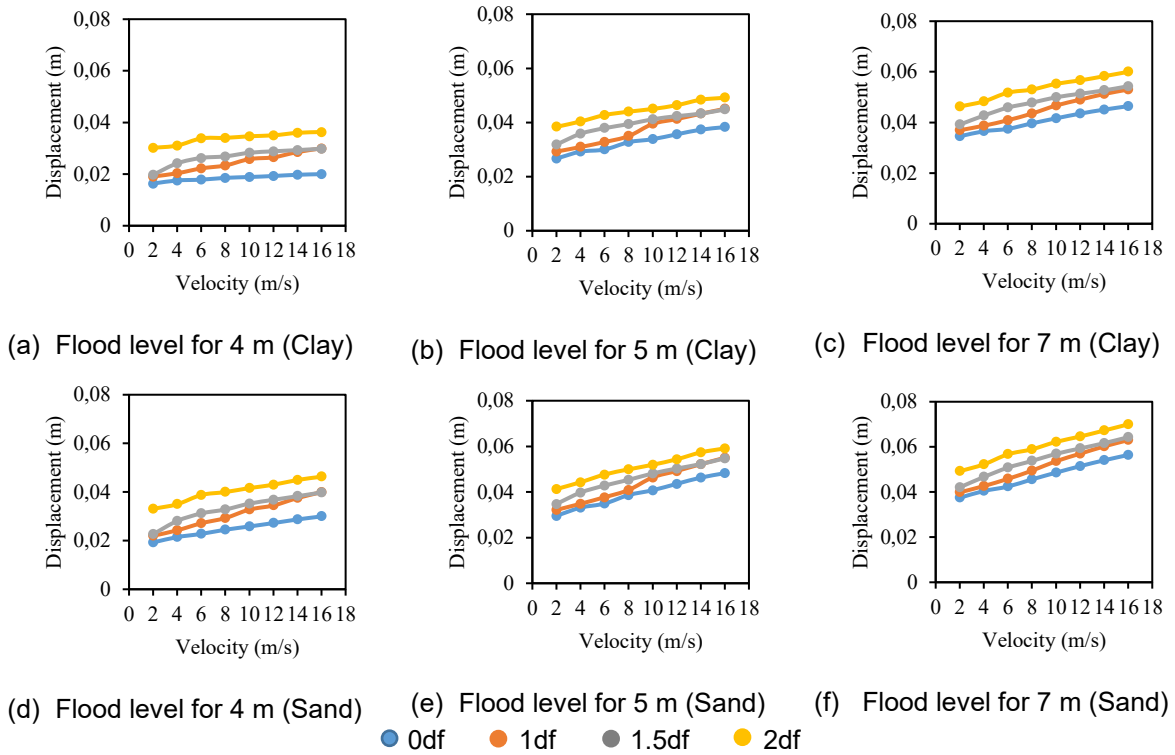


Figure 4. Graph of flood velocity versus pier displacement for every flood water level

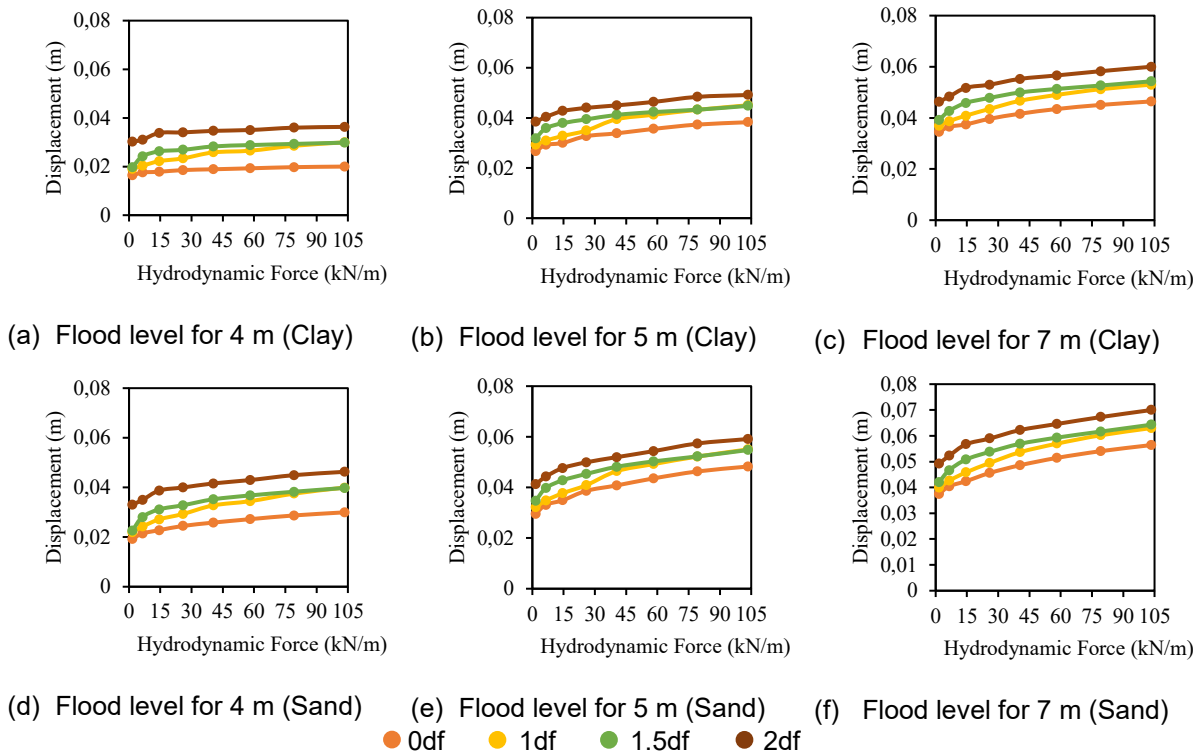


Figure 5. Graph of pier displacement versus hydrodynamic force for every flood water level

Hence, the linear/nonlinear flexural behavior of the pile will be governed by the thickness and location of the clayey or sandy stratum. This is consistent with the result in this

study where the increment of displacement from the ground C to type B ranges from 22-30 % especially for scour depth at 2df.

In overall, studies consistently show that denser soils, ground Type B (very stiff clay) have less displacement compared to ground Type C (medium dense sand). The consistent findings highlight the significant impact of soil properties on displacement behavior.

Statistical relationship between flood velocity, hydrodynamic force and pier displacement and comparison with previous works

To formalize the observed trends, the numerical results were fitted using a power-law model of the form $\delta = aV^b$, where δ is the pier-top displacement (m), V is the flood velocity (m/s), and a and b are regression coefficients. An analogous relationship $\delta = cF^d$, where F is the hydrodynamic line load (kN/m), was also considered. The parameters were obtained by ordinary least squares regression on log-log transformed data for each combination of soil type (very stiff clay, medium-dense sand), water level (4–7 m) and scour depth (0.0–2.4 m). The power-law model provides an excellent representation of the computed response, with an overall mean coefficient of determination $R^2 = 0.96$ and a mean mean-absolute-percentage error (MAPE) of approximately 2%. This confirms that the increase in pier displacement with flood intensity is smooth and monotonic, and can be efficiently captured by simple analytical expressions that are suitable for preliminary assessment and engineering design charts.

At the maximum scour depth of 2.4 m, the regression exponents show systematic differences between soil types. For the very stiff clay, the velocity exponent b lies in the range 0.09–0.13 across water levels, with R^2 between 0.96 and 0.97 and MAPE below 1.5%. For the sand case, b is consistently higher, between 0.16 and 0.17, with similar goodness-of-fit ($R^2 \approx 0.97$, MAPE $\approx 1.5\text{--}2.0\%$). These higher exponents indicate that, under identical hydraulic and scour conditions, pier displacement in sand grows more rapidly with velocity than in clay, reflecting the lower stiffness and higher flexibility of the sand–foundation system.

Using the fitted power-law relationships, pier displacements were predicted at a reference velocity of $V = 16$ m/s for the maximum scour condition. The results reveal that sand consistently produces larger displacements than clay, with increases between about 15% and 25% depending on water level. For example, at a water level of 4 m and scour depth of 2.4 m, the predicted displacement in sand is 0.045 m compared to 0.036 m in clay (approximately +25%). At higher water levels (5–7 m), the

difference reduces slightly but remains significant (around 19–16%). This quantitative comparison confirms the qualitative observation that sand foundations are more displacement-prone under extreme flood and scour conditions than very stiff clay.

The analytical trends observed in this study are consistent with earlier findings on bridge response under hydraulic loading and scour. HEC-18, [23], and [24] similarly reported that scour reduces lateral stiffness and leads to amplified pier deflection, which aligns with the increasing velocity exponent b obtained here as scour deepens. The influence of soil type on lateral deformation also agrees with previous SSI studies. [22][25], and [26] all showed that granular or sandy foundations experience larger lateral movement than stiff cohesive soils. This pattern matches the present results, where sand foundations produce 15–25% higher displacements than very stiff clay at the maximum scour depth.

Finally, the ability of a simple power-law model to capture displacement–velocity behaviour is consistent with flow–structure interaction formulations used in ASCE 7 and the empirical relationships proposed by [14]. The high goodness of fit ($R^2 > 0.95$) in this study reinforces the validity of using velocity-based analytical expressions for preliminary assessment under extreme flood events.

The findings of this study are in line with earlier research on the impact of scour and soil conditions on bridge performance during flood events. For example, [23] and [24] have shown that scour reduces the lateral stiffness of bridge foundations, which increases the potential for pier displacement—an effect also observed in this study. Similarly, research by [25] and [26], emphasized that foundations on sandy soils tend to experience more lateral movement compared to those on cohesive soils, due to lower stiffness. These trends mirror the displacement differences found between medium dense sand and very stiff clay in our results. Moreover, studies by [22] and [3] have highlighted the importance of incorporating soil–structure interaction into assessments of bridge vulnerability, particularly under combined flood and scour conditions. Building on these foundations, our study adds a new layer of insight by applying a detailed 3D finite element model, enabling a more nuanced and quantitative comparison of pier displacement across various soil types and flood intensities.

CONCLUSION

The study reveals a clear correlation between flood velocity, scour depth, and the resulting displacement of bridge piers. As flood velocity increases, the displacement of bridge piers rises consistently, with deeper scour depths exacerbating this effect. The findings show that bridge foundations on very stiff clay exhibit lower displacements compared to those on medium dense sand under similar conditions, indicating that stiff clay offers better resistance to hydrodynamic forces. The investigation also demonstrates a significant increase in pier displacement with increasing hydrodynamic forces across different scour depths. Notably, very stiff clay and medium dense sand foundations both show increasing displacement trends with rising scour depths and flood water levels. On the other hand, medium dense sand generally experiences higher displacements than stiff clay. This highlights the critical role of soil type in influencing the structural stability of bridge piers under hydrodynamic effects and local scour.

However, the present study limits its results to several hydraulic loadings, internal forces, local scour influences, and critical flow conditions. More water height, velocity, various scour depths, and the presence of debris or hydraulic loading need to be studied in order to measure more effects of the extreme flood on bridge response.

In relation to engineering, the following can be derived as the implications for enhancing bridge design and construction. The incorporation of SSI into flood resilience analysis allows for a more precise estimation of risks for flood-resistant areas, particularly in relation to bridges. Future work would include experimental validation, as well as extension of the modeling to variable rates of flow, debris strike, and Probabilistic Fragility Assessment. Model validation using lab testing, as well as comparisons based on operational experiences, would enhance the applicability of the model to real-life situations.

ACKNOWLEDGMENT

The funding for this study was provided by a grant from the Ministry of Higher Education of Malaysia (FRGS Grant: R0149-FRGS/1/2022/TK06/UPNM/02/3).

REFERENCES

- [1] M. Kosić, A. Anžlin, and V. Bau', "Flood Vulnerability Study of a Roadway Bridge Subjected to Hydrodynamic Actions, Local Scour and Wood Debris Accumulation," *Water (Switzerland)*, vol. 15, no. 1, pp. 1–26, Jan. 2023, doi: 10.3390/w15010129.
- [2] Z. Zhang, G. Lin, X. Yang, S. Cui, Y. Li, X. Shi and Z. Han, "A Review of Vibration-Based Scour Diagnosis Methods for Bridge Foundation," *Sustainability*, vol. 15, no. 10, art. 8210, 2023, doi: 10.3390/su15108210.
- [3] A. Anisha, A. Jacob, R. Davis, and S. Mangalathu, "Fragility functions for highway RC bridge under various flood scenarios," *Eng Struct*, vol. 260, pp. 1–12, Jun. 2022, doi: 10.1016/j.engstruct.2022.114244.
- [4] W. Cornwall, "Europe's deadly floods leave scientists stunned despite improvements, flood forecasts sometimes failed to flag risks along smaller streams," *Science (1979)*, vol. 373, no. 6553, pp. 372–373, Jul. 2021, doi: 10.1126/science.373.6553.372.
- [5] M. Loli, S. A. Mitoulis, A. Tsatsis, J. Manousakis, R. Kourkoulis, and D. Zekkos, "Flood characterization based on forensic analysis of bridge collapse using UAV reconnaissance and CFD simulations," *Science of the Total Environment*, vol. 822, pp. 1–18, May 2022, doi: 10.1016/j.scitotenv.2022.153661.
- [6] M. A. Zanini, F. Faleschini, N. Ademovic, L. J. Prendergast, K. Gavin, and M. P. Limongelli, "Structural Health Monitoring and Design Code compliance for performance assessment of bridges under scour and seismic hazards," Faculty of Civil Engineering, University of Zagreb, Dec. 2017, pp. 3.3-1-3.3-10. doi: 10.5592/co/bshm2017.3.3.
- [7] H. Kim, S. H. Sim, J. Lee, Y. J. Lee, and J. M. Kim, "Flood fragility analysis for bridges with multiple failure modes," *Advances in Mechanical Engineering*, vol. 9, no. 3, pp. 1–11, Mar. 2017, doi: 10.1177/1687814017696415.
- [8] A. Fioklou, A. Alipour, S. Brent, M. Phares, J. C. Ashlock, and P. Sarkar, "Performance assessment of reinforced concrete bridges under multi-hazard conditions and climate change effects," *Engineering Structures*, vol. 196, pp. 109325, 2019, doi: 10.1016/j.engstruct.2019.109325.
- [9] O. M. Nofal and J. W. van de Lindt, "Minimal building flood fragility and loss function portfolio for resilience analysis at the community level," *Water (Switzerland)*, vol. 12, no. 8, Aug. 2020, doi: 10.3390/w12082277.
- [10] S. A. Argyroudis and S. A. Mitoulis, "Vulnerability of bridges to individual and multiple hazards- floods and earthquakes," *Reliab Eng Syst Saf*, vol. 210, Jun. 2021, doi: 10.1016/j.ress.2021.107564.

[11] S. Stefanidou, A. Karatzetzou, G. Tsinidis, and S. A. Mitoulis, "Multi-hazard fragility assessment of bridges: Methodology and case study application," *Structures*, vol. 39, pp. 585–599, 2022, doi: 10.1016/j.istruc.2022.03.040.

[12] X. Guo, W. Chen, and Z. Q. Chen, "Probabilistic impact fragility analysis of bridges under Barge collision and local scour," *Applied Ocean Research*, vol. 134, May 2023, doi: 10.1016/j.apor.2023.103495.

[13] D. Zhang, W. Xiong, X. Ma, D. Zhou, and C. S. Cai, "Fragility evaluation of bridge shallow foundation piers under floods by coupling simulation in structural and hydraulic fields," *Ocean Engineering*, vol. 311, Nov. 2024, doi: 10.1016/j.oceaneng.2024.118952.

[14] J. Wang, K. Wei, and H. Cai, "Dynamic response of cylindrical bridge pier subjected to the impact of flash flooding considering the effect of soil–structure interactions," *Structures*, vol. 72, Feb. 2025, doi: 10.1016/j.istruc.2025.108199.

[15] X. Guo, W. Chen, and Z. Q. Chen, "Probabilistic impact fragility analysis of bridges under barge collision and local scour," *Applied Ocean Research*, vol. 134, pp. 103495, 2023, doi: 10.1016/j.apor.2023.103495.

[16] K. K. Marg, *Standard Specifications and Code of Practice for Road Bridges, Section II: Loads and Load Combinations*, 7th ed. New Delhi, India: Indian Roads Congress, 2017.

[17] S. Stefanidou, G. Tsinidis, and S. A. Mitoulis, "Multi-hazard fragility assessment of bridges under flood and earthquake loading," *Reliability Engineering & System Safety*, vol. 229, pp. 108828, 2023, doi: 10.1016/j.ress.2022.108828.

[18] B. J. Yian and Z. A. Talib, "Simulation of 2D ground movement due to tunnel excavation using Finite Element Method (FEM)," in *IOP Conference Series: Earth and Environmental Science*, Institute of Physics, vol. 1205, art. 012067, 2023, doi: 10.1088/1755-1315/1205/1/012067.

[19] A. Zaky, O. Özcan, and Ö. Avşar, "Seismic failure analysis of concrete bridges exposed to scour," *Eng Fail Anal*, vol. 115, Sep. 2020, doi: 10.1016/j.englfailanal.2020.104617.

[20] S. A. Mitoulis and S. A. Argyroudis, "Modelling soil–foundation–structure interaction for bridges subjected to combined flood and seismic hazards," *Soil Dynamics and Earthquake Engineering*, vol. 165, pp. 107577, 2023, doi: 10.1016/j.soildyn.2022.107577.

[21] M. Kosić, L. J. Prendergast, and A. Anžlin, "Analysis of the response of a roadway bridge under extreme flooding-related events: Scour and debris-loading," *Eng Struct*, vol. 279, pp. 1–15, Mar. 2023, doi: 10.1016/j.engstruct.2023.115607.

[22] A. Zaky, O. Özcan, and Ö. Avşar, "Numerical investigation of bridge foundations considering scour depth and nonlinear soil–structure interaction," *Engineering Failure Analysis*, vol. 146, pp. 107101, 2023, doi: 10.1016/j.englfailanal.2023.107101.

[23] M. Kosić, L. J. Prendergast, and A. Anžlin, "Analysis of the response of a roadway bridge under extreme flooding-related events: Scour and debris-loading," *Engineering Structures*, vol. 279, pp. 115607, 2023, doi: 10.1016/j.engstruct.2023.115607.

[24] D. Zhang, W. Xiong, X. Ma, D. Zhou, and C. S. Cai, "Fragility evaluation of bridge shallow foundation piers under floods by coupling simulation in structural and hydraulic fields," *Ocean Engineering*, vol. 311, pp. 118952, 2024, doi: 10.1016/j.oceaneng.2024.118952.

[25] A. Anisha, A. Jacob, R. Davis, and S. Mangalathu, "Flood fragility of reinforced concrete bridges considering hydrodynamic loading and uncertainty," *Engineering Structures*, vol. 260, pp. 114244, 2022, doi: 10.1016/j.engstruct.2022.114244.

[26] J. Wang, K. Wei, and H. Cai, "Dynamic response of cylindrical bridge pier subjected to the impact of flash flooding considering the effect of soil–structure interactions," *Structures*, vol. 72, pp. 108199, 2025, doi: 10.1016/j.istruc.2025.108199.

